Model uncertainties in computational viscoelastic linear structural dynamics

Rémi Capillon, Christophe Desceliers, Christian Soize

Model uncertainties in computational viscoelastic linear structural dynamics

R. Capillon[a], C. Desceliers[a,*], C. Soize[a]

[a] *Université Paris-Est, Laboratoire Modélisation et Simulation Multi-Echelle, MSME UMR 8208 CNRS, 5 bd Descartes, 77454 Marne-la-Vallée, France*

Abstract

This paper deals with the analysis of the propagation of uncertainties in computational linear dynamics for linear viscoelastic composite structures in the presence of uncertainties. In the frequency domain, the generalised damping matrix and the generalised stiffness matrix of the stochastic computational reduced-order model are random frequency-dependent matrices. Due to the causality of the dynamical system, these two frequency-dependent random matrices are statistically dependent and their probabilistic model involves a Hilbert transform. In this paper, a computational analysis of the propagation of uncertainties is presented for a composite viscoelastic structure in the frequency range.

Keywords: Uncertainty quantification, Viscoelastic, Nonparametric probabilistic approach, Structural dynamics, Hilbert transform, Kramers-Kronig relations, Reduced-order model

1. Introduction

In structural engineering, uncertainties have to be accounted for the design and the analysis of a structure using computational models. In the computational models, the sources of uncertainties are due to the model-parameters uncertainties, as well as the model uncertainties induced by modelling errors. In the probabilistic framework, uncertainty quantification has extensively be developed in the last two decades (see for instance [1–3]).

The objective of this paper is to present the numerical analysis of an extension (recently proposed in [4–6]) of the nonparametric probabilistic approach of uncertainties [7] in computational linear structural dynamics for viscoelastic composite structures in the frequency-domain. In the framework of linear viscoelasticity (see for instance [8, 9]) and in the frequency domain, the generalised damping matrix $[\mathcal{D}(\omega)]$ and the generalised stiffness matrix $[\mathcal{K}(\omega)]$ of the reduced-order computational model depend on frequency ω. The nonparametric probabilistic approach of uncertainties consists in modelling this two frequency-dependent generalised matrices by frequency-dependent random matrices $[\mathbf{D}(\omega)]$ and $[\mathbf{K}(\omega)]$ respectively. However, as these two matrices come from a causal dynamical system, the causality implies two compatibility equations, also known as the Kramers-Kronig relations [10, 11], involving the Hilbert transform [12]. A summary of the construction of the deterministic reduced-order computational model is presented in Section 2. Section 3 deals with the construction of the nonparametric probabilistic model using the Hilbert transform. In Section 4 a numerical example is presented.

*Corresponding author, Tel.: +33-1-60-95-7779 ; fax: +33-1-60-95-7799
E-mail address: christophe.desceliers@univ-paris-est.fr

2. Computational model in linear viscoelasticity

2.1. Linear viscoelastic constitutive equation

Let $\Omega = \Omega_e \cup \Omega_{ve}$ be an open, connected, and bounded domain of $\mathbb{R}^3$, constituted of two parts Ω_e and Ω_{ve}. The first part Ω_e is occupied by a purely elastic medium while the second part Ω_{ve} is occupied by a linear viscoelastic medium. In a cartesian frame $(\mathbf{e}_1, \mathbf{e}_2, \mathbf{e}_3)$, let $\mathbf{x} = (x_1, x_2, x_3)$ be the position vector of any point in Ω. Let $\mathbf{u}(\mathbf{x}, t)$ be the displacement field defined on Ω. The linearised strain tensor is denoted by $\{\varepsilon_{kh}\}_{hk}$ and the Cauchy stress tensor by $\{\sigma_{ij}\}_{ij}$, with i, j, k, and h in $\{1, 2, 3\}$. The theory of linear viscoelasticity is used in order to obtain the constitutive equation of the viscoelastic medium occupied by domain Ω_{ve}. For $t \leq 0$, the system is assumed to be at rest. In the time domain, the constitutive equation is then written as

$$\sigma(\mathbf{u}(\mathbf{x}, t)) = \int_0^t \mathcal{G}(\mathbf{x}, \tau) : \varepsilon(\dot{\mathbf{u}}(\mathbf{x}, t - \tau)) d\tau \,, \tag{1}$$

in which $\dot{\mathbf{u}}$ is the partial derivative of $\mathbf{u}$ with respect to t, where $t \mapsto \mathcal{G}(\mathbf{x}, t)$ is the relaxation function defined on $[0 + \infty[$ with values in the fourth-order tensor that satisfies the usual symmetry properties. Function $t \mapsto \mathcal{G}(\mathbf{x}, t)$ is differentiable with respect to t on $]0, +\infty[$ and its partial time derivative $t \mapsto \{\dot{\mathcal{G}}_{ijkh}(\mathbf{x}, t)\}_{ijkh}$ is assumed to be integrable on $[0\,, +\infty[$. At time $t = 0$, the initial elasticity tensor $\mathcal{G}(\mathbf{x}, 0)$ is positive definite. Consequently, Eq. (1) can be rewritten as

$$\sigma(\mathbf{u}(\mathbf{x}, \mathbf{t})) = \mathcal{G}(\mathbf{x}, 0) : \varepsilon(\mathbf{u}(\mathbf{x}, t)) + \int_{-\infty}^{+\infty} g(\mathbf{x}, \tau) : \varepsilon(\mathbf{u}(\mathbf{x}, t - \tau)) dt \,, \tag{2}$$

where fourth-order tensor $g(\mathbf{x}, t)$ is defined by $g(\mathbf{x}, t) = 0$, if $t < 0$ and $g(\mathbf{x}, t) = \dot{\mathcal{G}}(\mathbf{x}, t)$ if $t \geq 0$. Taking the Fourier transform with respect to t of both sides of Eq. (2), and introducing the real part $\widehat{g}^R(\mathbf{x}, \omega) = \Re e\{\widehat{g}(\mathbf{x}, \omega)\}$ and the imaginary part $\widehat{g}^I(\mathbf{x}, \omega) = \Im m\{\widehat{g}(\mathbf{x}, \omega)\}$, the constitutive equation in the frequency domain can be written as

$$\sigma(\widehat{\mathbf{u}}(\mathbf{x}, \omega)) = (a_0(\mathbf{x}) + a(\mathbf{x}, \omega) + \mathrm{i}\,\omega\, b(\mathbf{x}, \omega)) : \varepsilon(\widehat{\mathbf{u}}(\mathbf{x}, \omega)) \,, \tag{3}$$

where $a_0(\mathbf{x}) = \mathcal{G}(\mathbf{x}, 0)$ and where the components $a_{ijkh}(\mathbf{x}, \omega)$ and $b_{ijkh}(\mathbf{x}, \omega)$ of the fourth-order real tensors $a(\mathbf{x}, \omega)$ and $b(\mathbf{x}, \omega)$ are the viscoelastic coefficients that are such that

$$a(\mathbf{x}, \omega) = \widehat{g}^R(\mathbf{x}, \omega) \quad , \quad \omega\, b(\mathbf{x}, \omega) = \widehat{g}^I(\mathbf{x}, \omega) \,. \tag{4}$$

Since g is a causal function of time, the real part $\widehat{g}^R$ and imaginary part $\widehat{g}^I$ of its Fourier transform $\widehat{g}$ are related through a set of compatibility equations also known as the Kramers-Kronig relations [10, 11]. These relations involve the Hilbert transform [12] and are written as

$$\widehat{g}^R(\mathbf{x}, \omega) = \frac{1}{\pi}\, p.v \int_{-\infty}^{+\infty} \frac{\widehat{g}^I(\mathbf{x}, \omega')}{\omega - \omega'}\, d\omega', \quad \widehat{g}^I(\mathbf{x}, \omega) = -\frac{1}{\pi}\, p.v \int_{-\infty}^{+\infty} \frac{\widehat{g}^R(\mathbf{x}, \omega')}{\omega - \omega'} d\omega', \tag{5}$$

in which $p.v$ denotes the Cauchy principal value. From Eqs. (4) and (5), the following relation between the viscoelastic tensors $a(\mathbf{x}, \omega)$ and $b(\mathbf{x}, \omega)$ can then be deduced, for all $\omega > 0$,

$$a(\mathbf{x}, \omega) = \frac{\omega}{\pi}\, p.v \int_{-\infty}^{+\infty} \frac{b(\mathbf{x}, \omega')}{\omega - \omega'}\, d\omega' \,. \tag{6}$$

2.2. Computational model

The standard finite element method (see for instance [13, 14]) yields the computational model

$$(-\omega^2[\mathbb{M}] + i\omega[\mathbb{D}(\omega)] + [\mathbb{K}_0] + [\mathbb{K}(\omega)])\,\widehat{\mathbb{u}}(\omega) = \widehat{\mathbb{f}}(\omega) \,, \tag{7}$$

in which $\widehat{\mathbb{u}}(\omega)$ is the complex vector of the degrees of freedom, and where frequency-dependent matrices $[\mathbb{D}(\omega)]$, $[\mathbb{K}(\omega)]$ and matrix $[\mathbb{K}_0]$ are respectively related to $b(\mathbf{x}, \omega)$, $a(\mathbf{x}, \omega)$ and $a_0(\mathbf{x})$. Using Eq. (6), it is deduced that symmetric positive real matrix $[\mathbb{K}(\omega)]$ is such that

$$[\mathbb{K}(\omega)] = \frac{\omega}{\pi}\, p.v \int_{-\infty}^{+\infty} \frac{1}{\omega - \omega'} [\mathbb{D}(\omega)]\, d\omega' \tag{8}$$

2.3. Reduced-order computational model

As suggested in [5], the reduced-order computational model is constructed by using the reduced basis represented by the first N modes associated with the first N positive eigenvalues of the underlying undamped mechanical system for which the mass matrix is $[\mathbb{M}]$ and the stiffness matrix is $[\mathbb{K}_0]$. The reduced-order computational model is then written as

$$(-\omega^2[\mathcal{M}] + i\omega\,[\mathcal{D}(\omega)] + [\mathcal{K}_0] + [\mathcal{K}(\omega)])\,\widehat{\mathbf{q}}(\omega) = \widehat{\mathbf{f}}(\omega)\,, \tag{9}$$

where the frequency-dependent full $(N \times N)$ real matrices $[\mathcal{D}(\omega)]$ and $[\mathcal{K}(\omega)]$ are symmetric positive and are such that

$$[\mathcal{K}(\omega)] = \frac{\omega}{\pi}\; p.v \int_{-\infty}^{+\infty} \frac{1}{\omega - \omega'}[\mathcal{D}(\omega)]d\omega' \quad , \quad \omega \geq 0\,. \tag{10}$$

3. Stochastic reduced-order computational model

For N fixed, the nonparametric probabilistic approach of uncertainties consists in substituting in Eqs. (9) and (10), the deterministic matrices $[\mathcal{M}]$, $[\mathcal{D}(\omega)]$, $[\mathcal{K}_0]$, and $[\mathcal{K}(\omega)]$, by the $(N \times N)$ real random matrices $[\mathbf{M}]$, $[\mathbf{D}(\omega)]$, $[\mathbf{K}_0]$, and $[\mathbf{K}(\omega)]$ respectively, in preserving the positive-definiteness property of $[\mathbf{M}]$, $[\mathcal{D}(\omega)]$, $[\mathbf{K}_0]$, and the positiveness property of $[\mathbf{K}(\omega)]$. Consequently $\widehat{\mathbf{q}}(\omega)$ becomes the random vectors $\widehat{\mathbf{Q}}(\omega)$ such that

$$(-\omega^2[\mathbf{M}] + i\omega\,[\mathbf{D}(\omega)] + [\mathbf{K}_0] + [\mathbf{K}(\omega)])\,\widehat{\mathbf{Q}}(\omega) = \widehat{\mathbf{f}}(\omega)\,, \tag{11}$$

$$[\mathbf{K}(\omega)] = \frac{2\,\omega}{\pi}\; p.v \int_{0}^{+\infty} \frac{1}{1 - u^2}[\mathbf{D}(\omega u)]\,du \quad , \quad \omega \geq 0\,. \tag{12}$$

Furthermore, Eq. (12) means that the probabilistic model of random matrix $[\mathbf{K}(\omega)]$ is completely defined by the probabilistic model of random matrix $[\mathbf{D}(\omega)]$ and consequently, the two random matrices are not statistically independent such that the probabilistic model for random matrix $[\mathbf{K}(\omega)]$ allows satisfying almost-surely the causality principle and will be referred as the probabilistic model with almost-sure causality. Consequently, only the probabilistic models of random matrices $[\mathbf{M}]$, $[\mathbf{K}_0]$ and $[\mathbf{D}(\omega)]$ have to be constructed.

In the framework of the nonparametric probabilistic approach of uncertainties, these random matrices are statistically independent and they are constructed as explained in [4, 7]. Their level of uncertainty is respectively controlled by parameters δ_M, δ_K, $\delta_M < (\frac{N+1}{N+5})^{1/2}$. On an other hand, if the causality principle was not taken into account for the construction of the stochastic model of random matrix $[\mathbf{K}(\omega)]$, then the stochastic model that would be constructed would be causal in average but would not be almost-surely causal. Such a model would be erroneous from the point of view of the theory of physically realizable systems. In the following, such an erroneous stochastic construction will be referred as the probabilistic model with a causality in mean. Such a model can be constructed by rewriting Eq. (11) as

$$([\mathbf{M}] + i\omega[\mathbf{D}(\omega)] + [\widetilde{\mathbf{K}}(\omega)])\,\widehat{\mathbf{Q}}(\omega) = \widehat{\mathbf{f}}(\omega)\,, \tag{13}$$

where $[\widetilde{\mathbf{K}}(\omega)] = [\mathbf{K}_0] + [\mathbf{K}(\omega)]$. The random matrices $[\mathbf{M}]$, $[\mathbf{K}(\omega)]$ and $[\mathbf{D}(\omega)]$ are statistically independent and are constructed as explained in [4, 7]. Their level of uncertainty is respectively controlled by parameters δ_M, δ_K, $\delta_M < (\frac{N+1}{N+5})^{1/2}$.

4. Numerical example and results

4.1. Description of the numerical model

As an example, a composite structure is studied in the Low-Frequency range. It is a thin multilayered plate of length $L = 1$ m, width $W = 0.3$ m and thickness $H = 0.1$ m, under a nodal load of $F = 1$ N applied in direction the vertical direction $\mathbf{e}_3$ at the point located at (0.5067 m, 0.1565 m, 0.1 m) (see Fig. 1). Let $\widehat{u}_k(\omega) = \{\widehat{\mathbb{u}}(\omega)\}_k$ be the k-th component of the response calculated with computational model. The numbering of degrees of freedom is such that,

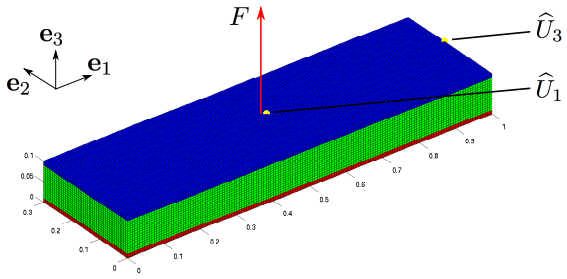

Figure 1: Finite element mesh of the plate with force applied $F = 1$ N and observation dofs $\widehat{u}_1$ and $\widehat{u}_3$.

for $k = 1$, $\widehat{U}_k(\omega)$ is related to the degree of freedom that is submitted to the external force F.The three layers are made up of a homogenous elastic medium occupying domain Ω_e that is sandwiched between two homogenous viscoelastic media occupying the domain $\Omega_{ve} = \Omega_1 \cup \Omega_2$ in which the domain Ω_1 is the upper layer and the domain Ω_2 is the lower layer. For the elastic medium, the material is assumed to be isotropic with Young's modulus $E = 210$ GPa, Poisson's ratio $\nu = 0.3$, and a density $\rho = 7,850$ kg/m^3. Its thickness is $h = 4H/5$ in which H is the total thickness of the plate. For the viscoelastic homogenous medium occupying domain Ω_k, with $k = 1, 2$, the material is assumed to be isotropic with a Poisson ratio $\nu^{(k)}$ and a time-dependent viscoelastic coefficient $E^{(k)}(t)$. Let $\widehat{E}^{(k)}(\omega)$ be the Fourier transform of $E^{(k)}(t)$. In the case of a single-branch generalised Maxwell model, we have

$$\widehat{E}_k(\omega) = E_\infty^{(k)} + \frac{E_1^{(k)}(\tau_1^{(k)}\omega)^2}{1 + (\tau_1^{(k)}\omega)^2} + i\omega\frac{E_1^{(k)}\tau_1^{(k)}}{1 + (\tau_1^{(k)}\omega)^2} \,. \tag{14}$$

The viscoelastic coefficients used in the simulations are $\nu^{(1)} = 0.27$, $\nu^{(2)} = 0.47$, $E_\infty^{(1)} = 240$ GPa, $E_\infty^{(2)} = 220$ GPa, $E_1^{(1)} = 126.5$ GPa, $E_1^{(2)} = 50$ GPa, $\tau_1^{(1)} = 7.351 \times 10^{-2}$s and $\tau_1^{(1)} = 1.103 \times 10^{-1}$s.

4.2. Analysis of the stochastic model

Hereinafter, the two random models with almost-sure causality (see Eqs. (11) and (12)) and with the causality in mean (see Eq. (13)) are compared. It is assumed that $[\mathbf{M}]$ remains deterministic ($\delta_M = 0$), and that $\delta_K = 0.15$ and $\delta_D = 0.7$. The numbering of degrees of freedom is such that, for $k = 3$, $\widehat{U}_k(\omega)$ is related to the degree of freedom in direction $\mathbf{e}_1$ of the node located, respectively, at (0.5067 m, 0.1630 m, 0.1 m) (see Fig. 1).

Let $u \mapsto p_{|\widehat{U}_3^{(N)}|}(u;\omega)$ be the probability density function of $|\widehat{U}_3^{(N)}(\omega)|$. Figs. 2, 3, and 4 display the graphs of $u \mapsto p_{|\widehat{U}_3|}(u; 2\pi\nu)$ at frequencies $\nu = 2$ Hz, $\nu = 200$ Hz, and $\nu = 400$ Hz, for the two probabilistic models with almost-sure causality (red line) and with causality in mean (blue line). Figs. 2 to 4 show that the probabilistic model with causality in mean does not give a good prediction (except for the low frequency 2 Hz that corresponds to a quasistatic response because the fundamental eigenfrequency is about 3 Hz).

5. Conclusions

In the framework of the nonparametric probabilistic approach of uncertainties, a new stochastic modelling has been proposed for taking into account uncertainties in the computational models of linear viscoelastic dynamical structures. This method is based on the construction of a compatibility equation that allows for satisfying the causality principle for the stochastic dynamical system in order to obtain compatible probabilistic model of the random stiffness matrix and the random damping matrix at each frequency point of analysis. A numerical example has been presented for analysing the propagation of uncertainties in a computational model of a composite viscoelastic structure. The results obtained show that it is very important to construct a probabilistic model which satisfies the causality principle.

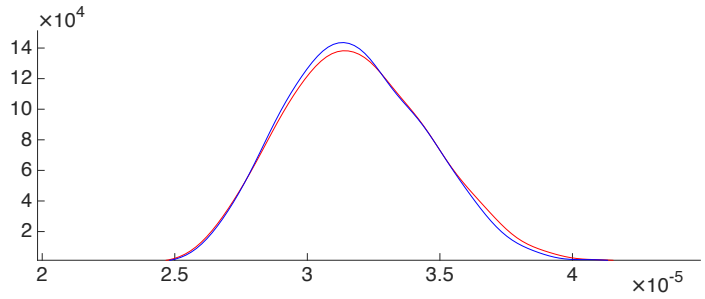

Figure 2: Graph of $u \mapsto p_{|\widehat{U}_3|}(u; 2\pi\nu)$ at frequency $\nu = 2$ Hz. Probabilistic model with almost-sure causality (red line) and probabilistic model with causality in mean (blue line).

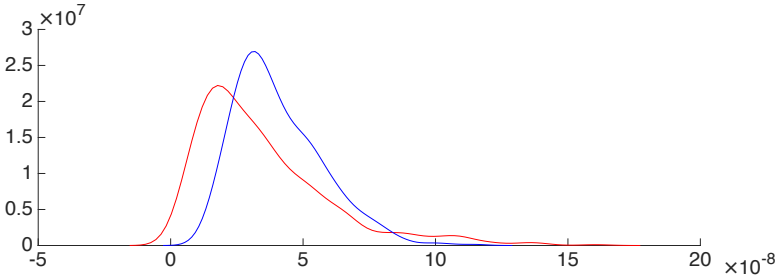

Figure 3: Graph of $u \mapsto p_{|\widehat{U}_3|}(u; 2\pi\nu)$ at frequency $\nu = 200$ Hz. Probabilistic model with almost-sure causality (red line) and probabilistic model with causality in mean (blue line).

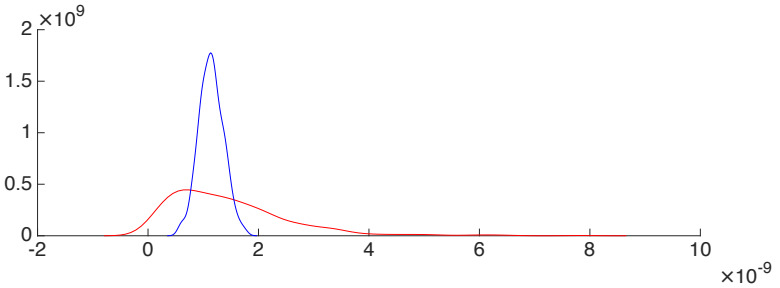

Figure 4: Graph of $u \mapsto p_{|\widehat{U}_3|}(u; 2\pi\nu)$ at frequency $\nu = 400$ Hz. Probabilistic model with almost-sure causality (red line) and probabilistic model with causality in mean (blue line).

References

[1] R.Ghanem, P.D.Spanos, Stochastic Finite Elements : A Spectral Approach, Springer-Verlag, NewYork, 1991 (Revised edition, Dover Publications, New York, 2003).

[2] R. Mace, W. Worden, G. Manson, Uncertainty in structural dynamics, J. Sound Vib. 288(3) (2005) 431-790.

[3] G.I.Schueller (Ed.), Computational methods in stochastic mechanics and reliability analysis, Comput. Methods Appl. Mech. Engrg. 194(12-16) (2005) 1251-1795.

[4] C. Soize, I.E. Poloskov, Time-domain formulation in computational dynamics for linear viscoelastic media with model uncertainties and stochastic excitation, Computers and Mathematics with Applications 64(11) (2012) 3594-3612.

[5] R. Ohayon, C. Soize, Advanced Computational Vibroacoustics, Cambridge University Press, New York, 2014.

[6] R. Capillon, C. Desceliers, C. Soize., Uncertainty quantification in computational linear structural dynamics for viscoelastic composite structures, Computer Methods in Applied Mechanics and Engineering, 305 (2016) 154-172.

[7] C. Soize, Uncertainty Quantification. An Accelerated Course with Advanced Applications in Computational Engineering, Springer, New York, 2017.

[8] C. Truesdell, Encyclopedia of Physics, Vol. VIa/3, Mechanics of Solids III, Springer-Verlag, Berlin, 1973.

[9] R.M. Christensen, Theory of Viscoelasticity (Second Edition), Academic Press, 1982.

[10] H.A. Kramers, La diffusion de la lumiere par les atomes, Atti Cong. Intern. Fisica, (Transactions of Volta Centenary Congress) Como 2 (1927) 545-557.

[11] R.D. Kronig, On the theory of dispersion of X-rays, J. Opt. Soc. Amer. 12(6) (1926) 547-557.

[12] A. Papoulis, Signal Analysis, McGraw-Hill, New York, 1977.

[13] K.J. Bathe. *Finite Element Procedures*, Prentice Hall, 1996.

[14] O.C. Zienkiewicz, R.L. Taylor. *The Finite Element Method Set (Sixth Edition)*, Butterworth-Heinemann, 2005.